Transient Electromagnetic Fields Near Large Earthing Systems

Leonid D. Grcev
University "St. Cyril and Methodius," Skopje, Republic of Macedonia

Frank E. Menter
SIEMENS AG, Erlangen, Germany

***Abstract*—Electromagnetic compatibility studies require knowledge of transient voltages that may be developed near earthing systems during lightning discharge, since such voltages may be coupled to sensitive electronic circuits. For such purpose accurate evaluation of transient electric field near to and/or at the surface of the grounding conductors is necessary. In this paper, a procedure for computation of transient fields near large earthing systems, as a response to a typical lightning current impulse, based on computational methodology developed in the field of antennas, is presented. Computed results are favorably compared with published measurement results. The model is applied to check the common assumption that the soil ionization can be neglected in case of large earthing systems. Presented results show that the soil ionization threshold is met and exceeded during typical lightning discharge in a large earthing system.**

I. Introduction

Extended meshed earthing systems are used in large installations, such as: power stations or plants, to ensure safety to the personnel and the equipment. They also provide reference voltages for electrical and electronic systems. Local inequalities of the reference voltages, and induced or conducted transient voltages coupled to circuits with sensitive electronic systems, during lightning discharge and power system faults, can be a cause for their malfunction or destruction. Voltages in general case are path dependent on higher frequencies, and have to be evaluated as integral of the electric field vector between two points along a given path. Consequently, electromagnetic compatibility (EMC) and lightning protection studies require knowledge of the spatial and temporal distribution of electromagnetic fields near the earthing systems in case of lightning and power system faults.

In this paper, the transient problem is first solved by a formulation in the frequency domain. The time domain response is then obtained by application of a suitable Fourier inversion technique. The grounding system is assumed to be a network of connected straight cylindrical metallic conductors with arbitrary orientation and finite conductivity, Fig. 1. The conductors are subject to the thin-wire approximation, assuming that their radiuses are much smaller than the wavelength and lengths are much greater than the radiuses. This assumption enables to approximate the total current in the conductors as filamentary line current in the conductors' axis. The soil is modeled as linear and homogeneous half-space characterized by conductivity, permittivity and permeability constants.

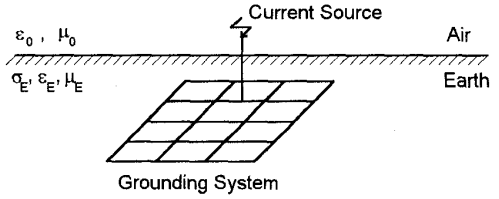

Fig. 1. Physical Situation.

II. Longitudinal Current Distribution

The assumptions introduced in the previous section enable application of efficient computational methodology developed in the field of antennas [1]. The first step is to compute the current distribution, as a response to injected current at arbitrary points on the conductor network, in frequency domain. First, current sampling points are defined at each corner or bending point, at each junction where several conductors intersect and at the conductors end points, Fig. 2. These current sampling points divide the network of conductors into a number of fictitious segments. To approximate the current between the sampling points, that is along segments, filamentary current distribution in axes of every two neighbor segments is defined. Such distributions can be considered as filamentary electrical dipoles with current that is zero at the end points and that rises sinusoidally to a maximum at the junction point between the two segments, so called "sinusoidal dipoles" [1]. Also to approximate the current along the segment with the injection point, one "sinusoidal monopole" is added, Fig. 2. The distribution of the longitudinal current $I(\ell)$ at a point ℓ on the whole conductor network can be defined by an array of M overlapped sinusoidal dipoles and monopoles, Fig. 2:

$$I(\ell) = \sum_{k=0}^{M} I_k F_k(\ell) \tag{1}$$

Manuscript received July 10, 1995.

L. D. Grcev, fax +389-91-364-262; F. E. Menter, phone +49-9131-7-20248, fax +49-9131-7-26961.

The first author gratefully acknowledges support by the Ministry of Science of Republic of Macedonia.

0018-9464/96$05.00 © 1996 IEEE

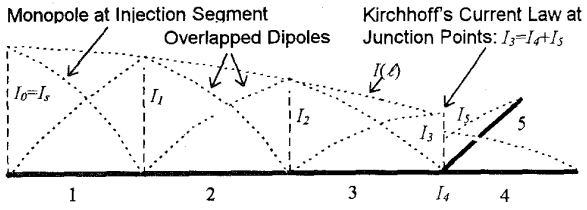

Fig. 2. Approximation of Current Along Segmented Conductor Network.

where I_k are current samples. The normalized function of the current distribution over the length of one sinusoidal dipole $F_k(\ell)$ is [1]:

$$F_k(\ell)=\frac{P_{k1}(\ell)\sinh\gamma_E(\ell-\ell_{k1})}{\sinh\gamma_E d_{k1}}+\frac{P_{k2}(\ell)\sinh\gamma_E(\ell_{k3}-\ell)}{\sinh\gamma_E d_{k2}} \quad (2)$$

$$P_{k1}(\ell)=\begin{cases}1, & \ell_{k1}\le\ell\le\ell_{k2}\\ 0, & \text{elsewhere}\end{cases},\quad P_{k2}(\ell)=\begin{cases}1, & \ell_{k2}\le\ell\le\ell_{k3}\\ 0, & \text{elsewhere}\end{cases}$$

$$\gamma_E^2=-\omega^2\mu_E\underline{\varepsilon}_E=-\omega^2\mu_E\left(\varepsilon_E+\frac{\sigma_E}{j\omega}\right)$$

Here ℓ is a point at the conductor axis, and ℓ_{k1}, ℓ_{k2}, and ℓ_{k3}, are the first, the middle, and the last point of the k^{th} sinusoidal dipole, respectively. Lengths of the first and the second segment of the k^{th} sinusoidal dipole are denoted by d_{k1} and d_{k2}. Constants of conductivity, permittivity and permeability of the soil are denoted by σ_E, ε_E and μ_E, respectively. Additional current sampling points may be added along segments depending on ability of (1) to approximate accurately the real current variation along conductors. Segments' length d_k have to be shorter than the wavelength in the soil (actual number of segments per wavelength has to be determined by the convergence of the results). The Kirchhoff's current law is explicitly enforced on all segments' junction points, Fig. 2. It should be noted that the time-variation $\exp(j\omega t)$ is suppressed.

Longitudinal current distribution (1) may be evaluated from the system of equations:

$$[Z]\cdot[I]=[-Z_0 I_s] \quad (3)$$

where the elements of the column matrix $[I]$ are unknown current samples. Elements of $[Z]$ are mutual impedances between sinusoidal dipoles. Elements of $[-Z_0 I_s]$ are mutual impedances between sinusoidal dipoles and the sinusoidal monopole on the injection segment multiplied by excitation current I_s. Elements of $[Z]$ are[1]:

$$z_{mn}=\int_{(n)}F_n(\ell_n)\vec{\ell}_n\cdot\vec{E}_m d\ell-\frac{Z_s}{2\pi a}\int_{(m,n)}F_m(\ell_m)F_n(\ell_n)d\ell \quad (4)$$

Here $\vec{\ell}_n\cdot\vec{E}_m$ is tangential axial component of the electric field due to current in m^{th} dipole at the surface of the segments of n^{th} dipole. Radius of conductors is denoted by a, and region (m, n) is segments shared by m^{th} and n^{th} dipole. Z_s is the surface impedance defined in [2] as the ratio of the tangential electric field strength at the surface of the conductor to the current density which flows as a result of that tangential electric field. If σ_C, ε_C and μ_C represent the common conductance, permittivity and permeability of the conductors, then [3]:

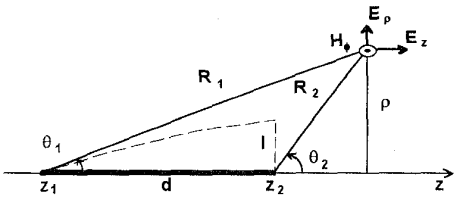

Fig. 3. Local Coordinate System

$$Z_s=\frac{\lambda_C}{2\pi a(\sigma_C+j\omega\varepsilon_C)}\cdot\frac{J_0(\lambda_C)}{J_1(\lambda_C)} \quad (5)$$

Here $\lambda_C\approx\omega^2(\mu_C\underline{\varepsilon}_C-\mu_E\underline{\varepsilon}_E)$. The Bessel functions of the first kind of order zero and one are denoted J_0 and J_1, respectively. To determine z_{mn} (4) it is necessary to evaluate the electric field due to the assumed current distribution.

III. Rigorous Expressions for Electromagnetic Field

The rigorous expressions for the ρ- and z-components of the electric field and the ϕ-component of the magnetic field at a near point due to a sinusoidal monopole (with zero current at z_1 and I at z_2), in a local cylindrical coordinate system illustrated in Fig. 3, are [1]:

$$E_\rho=\eta_E\frac{C}{\rho}I\,[-\exp(-\gamma_E R_2)\sinh\gamma_E d-\exp(-\gamma_E R_1)\cos\theta_1 \quad (6)$$
$$-\exp(-\gamma_E R_2)\cosh\gamma_E d\cos\theta_2]$$

$$E_z=\eta_E CI\left[-\frac{1}{R_2}\exp(-\gamma_E R_2)\cosh\gamma_E d-\frac{1}{R_1}\exp(-\gamma_E R_1)\right]$$

$$H_\phi=\frac{C}{\rho}I\,[-\exp(-\gamma_E R_1)-\exp(-\gamma_E R_2)\sinh\gamma_E d\cos\theta_2$$
$$+\exp(-\gamma_E R_2)\sinh\gamma_E d]$$

$$\eta_E=\sqrt{\mu_E/\underline{\varepsilon}_E},\quad C=\frac{1}{4\pi\sinh\gamma_E d}$$

where various quantities are illustrated in Fig. 3 or are given in (2). The electric field at a point near the grounding system is the sum of contributions from the overlapped sinusoidal current sources in all segments. Formulas (6) are valid in unbounded homogeneous medium. The effect of earth's surface is taken into account by the modified image theory [4].

IV. Modified Image Theory

The electric field radiated by a current source placed below or above the earth's surface can be evaluated by the modified method of images [4]. The following cases can be considered for the position of the source and observation point.

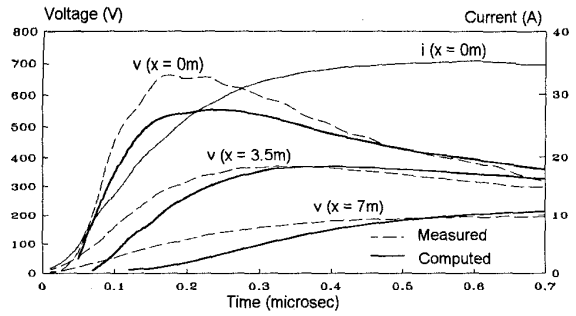

Fig. 4. Measured and Computed Transient Voltage to Remote Reference Ground at Three Points Along Horizontal Copper Wire (15 m length, 12 mm radius, 0.6 m depth, 70 Ωm soil's resistivity, 15 soil's relative permittivity).

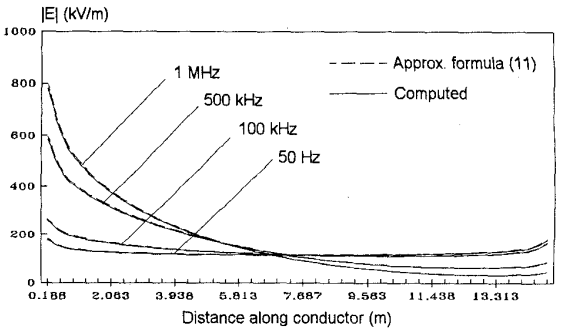

Fig. 5. Normal component of the electric field at the surface of 15m long horizontal conductor.

Source and observation point in the same medium: The electric field can be evaluated as a sum of the field of the current source I and its image I':

$$I'_E = \frac{\underline{\varepsilon}_E - \varepsilon_0}{\underline{\varepsilon}_E + \varepsilon_0} I_E \,, \quad I'_A = \frac{\varepsilon_0 - \underline{\varepsilon}_E}{\underline{\varepsilon}_E + \varepsilon_0} I_A \tag{7}$$

where ε_0 is permittivity of vacuum, and subscripts E and A, denote the position in earth and air, respectively.

Source and observation point in different mediums: The electric field can be evaluated as field due to the modified current source I'':

$$I''_A = \frac{2\varepsilon_0}{\underline{\varepsilon}_E + \varepsilon_0} I_A \,, \quad I''_E = \frac{2\underline{\varepsilon}_E}{\underline{\varepsilon}_E + \varepsilon_0} I_E \tag{8}$$

V. Verification of the Computer Model

A. Comparison with Field Measurements

Recordings from field measurements of transient voltages to remote ground performed by the Electricite de France (EDF) [5] are used to verify the model. Fig. 4 shows the oscillograms of recorded current impulse injected at the end point of 15 m long horizontal ground wire and transient voltage to remote ground at three points along the wire. Computations are made by integrating the electric field from the surface of the conductor to the remote reference ground. The measured voltages were always higher during the current rise than the corresponding values of the computation, since the measured voltages are likely to be amplified by some remaining inductive voltage drop during the wave front along the 60m long voltage divider [5], that was not included in the simulation.

B. Checking Electric Field Computations by Approximate Formula

In case of linear conductor the normal component of the electric field at a point on the surface E_n and is found by constructing a cylinder of radius a equal to the radius of the conductor and differential length $d\ell$. Then Gauss' law yields:

$$Q' = \frac{1}{d\ell} \oiint_S \vec{D} \cdot d\vec{s} \approx 2\pi a \underline{\varepsilon}_E E_\rho + \iint_{S_1} \frac{\partial E_\ell}{\partial \ell} ds \tag{9}$$

where Q' is charge per unit length and S is the total surface of the cylinder and S_1 is one of its end faces. Using the equation of continuity

$$Q' = -\frac{1}{j\omega} \frac{\partial I}{\partial \ell} \tag{10}$$

and noting that the second term of (9) is dominant at the conductors' open ends and is negligible elsewhere, (9) and (10) yield for E_n along the conductor:

$$E_n \approx -\frac{1}{2\pi a j\omega \underline{\varepsilon}_E} \frac{\partial I}{\partial \ell} \tag{11}$$

Here I is the longitudinal current and ℓ is coordinate along the axis of the conductor.

Figure 5 shows the intensity of the normal component of the electric field at the surface of the conductor along its length computed by the computer program and the approximate formulae (11). A 15 m long horizontal conductor is energized by injection of 1 kA steady-state time-harmonic current on several frequencies from 50 Hz to 1 MHz (parameters of the conductor and soil are identical with the corresponding in Fig. 4). Excellent agreement between the results is obtained.

VI. Example of Application: Soil Ionization Threshold in Large Grounding Grids

As an example for analysis, a 60 m by 60 m square ground grid with 10 m by 10 m meshes, made of copper conductors with 1.4 cm diameter, and buried at a depth of 0.5 m, is chosen. The soil is assumed to be homogeneous with a resistivity 1000 Ωm, a relative permittivity 9 and a relative permeability 1. A typical double-exponential lightning current impulse [6]–[8], with peak value 10 kA, time-to-maximum 1 μs and time-to-half-maximum 50 μs, is fed at a point in the corner of the grid.

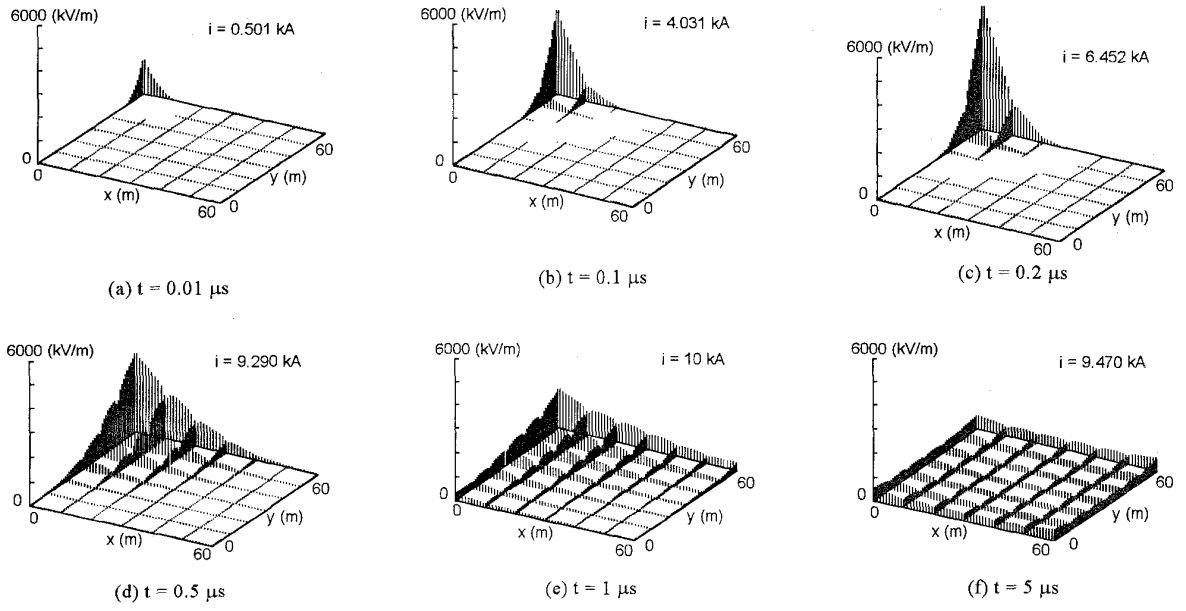

Fig. 6. Normal Component of the Electric Field at the Surface of 60 m by 60 m Grounding Grid Conductors as a Response to Injected Double-Exponential 1 μs / 50 μs 10 kA Crest Surge (Corner Injection, Soil: ρ = 1000 Ωm, ε_r = 9).

This example is chosen since it was also used in [6]–[8], and is suitable for comparison. Possibility of soil ionization is not taken into account in [6]–[8]. It is in accordance to the widely accepted assumption that the soil ionization can be neglected in large earthing systems. It is usually assumed that due to the long length of buried conductors the electric field in soil is lower than the critical breakdown threshold.

In this paper computations are presented to check if the soil ionization threshold is met or exceeded in the chosen case. Fig. 6 shows temporal and spatial evolution of the electric field at the surface of the grounding grid conductors at six moments of time. Values of the excitation current are also shown in the figures. Presented model enables detailed insight in the large grounding grid behavior in the early time of the transient response.

It is shown that electric field at the surface of the conductors is developed first near the injection point and propagates over the grounding grid surface by a finite speed. Maximum values occur early, at about 0.2 μs, compared to the maximum of the excitation current at 1 μs. The transient period ends at about 1.5 μs, when distribution typical for dc excitation is developed (Fig. 6f).

The presented results show that the soil ionization threshold (from 300 kV/m to 1000 kV/m [9]) is exceeded during the transient period. This indicates that contrary to the usual assumption, the phenomenon of the soil ionization has to be taken into account in the analysis of transient performance of large grounding systems subjected to typical lightning current impulses.

This also indicates that the domain of applicability of the presented method is limited to cases when the soil ionization threshold is not met, that is, to excitation impulses with lower peak values. This limitation also applies to other computer models that neglect this phenomenon, for example [6]–[8].

References

[1] J. H. Richmond, "Radiation and Scattering by Thin-Wire Structures in the Complex Frequency Domain," in *Computational Electromagnetics*, E. K. Miller, Ed., New York: IEEE Press, 1992 [Report No. 2902-10, ElectroScience Laboratory, The Ohio State University, May 1974].

[2] E. C. Jordan and K. G. Balmain, *Electromagnetic Waves and Radiating Systems*, New Jersey: Prentice-Hall, 1968.

[3] J. A. Stratton, *Electromagnetic Theory*, New York: McGraw-Hill, 1941.

[4] T. Takashima, T. Nakae, and R. Ishibashi, "Calculation of Complex Fields in Conducting Media," *IEEE Transactions on Electrical Insulation*, Vol. 15, 1980, pp. 1-7.

[5] H. Rochereau, "Response of Earth Electrodes when Fast Fronted Currents are Flowing Out," *EDF Bulletin de la Direction des Etudes et Recherches*, serie B, no. 2, 1988, pp. 13-22.

[6] A. P. Meliopoulos and M. G. Moharam, "Transient Analysis of Grounding Systems," *IEEE Transactions on Power Apparatus and Systems*, Vol. PAS-102, Feb. 1983, pp. 389-399.

[7] L. Grcev, "Computation of Transient Voltages Near Complex Grounding Systems Caused by Lightning Currents," *Proceedings of the IEEE 1992 International Symposium on Electromagnetic Compatibility*, 92CH3169-0, pp. 393-400.

[8] W. Xiong and F. Dawalibi, "Transient Performance of Substation Grounding Systems Subjected to Lightning and Similar Surge Currents," *IEEE Transactions on Power Delivery*, Vol. 9, July 1994, pp. 1421-1427.

[9] A. M. Mousa, "The Soil Ionization Gradient Associated with Discharge of High Currents into Concentrated Electrodes," *IEEE Transactions on Power Delivery*, Vol. 9, July 1994, pp. 1669-1677.